

Structures, Electron Affinities, and Harmonic Vibrational Frequencies of the Simplest Alkyl Peroxyl Radicals and Their Anions

Wenguo Xu* and Gaoyu Lu

The Institute for Chemical Physics, Beijing Institute of Technology, Beijing 100081, People's Republic of China

Received: December 19, 2007; Revised Manuscript Received: April 20, 2008

The molecular structures and electron affinities of the R-OO/R-OO⁻ (R = CH₃, C₂H₅, *n*-C₃H₇, *n*-C₄H₉, *n*-C₅H₁₁, *i*-C₃H₇, *t*-C₄H₉) species have been determined using seven different density functional or hybrid Hartree–Fock density functional methods. The basis set used in this work is of double- ζ plus polarization quality with additional diffuse s-type and p-type functions, denoted DZP++. The geometries are fully optimized with each density functional theory method. Harmonic vibrational frequencies were found to be within 3.1% of available experimental values for most functionals. Two different types of the neutral–anion energy separations reported in this work are the adiabatic electron affinity and the vertical detachment energy. The most reliable adiabatic electron affinities obtained at the DZP++ BP86 level of theory are 1.150 (CH₃OO), 1.124 (C₂H₅OO), 1.146 (*n*-C₃H₇OO), 1.173 (*n*-C₄H₉OO), 1.184 (*n*-C₅H₁₁OO), 1.145 (*i*-C₃H₇OO), and 1.114 eV (*t*-C₄H₉OO). Compared with the experimental values, the average absolute error of the BPW91 method is 0.05 eV.

Introduction

During the past decades, alkyl peroxyl radicals (ROO) have generated continued interest because of their potential significance in atmospheric chemistry, combustion chemistry, biochemistry, and environmental chemistry, and there have been a large number of reports on their kinetics, mechanisms, and spectroscopies.^{1–12} Alkyl peroxyl radicals are critical reactive intermediates in the generation of photochemical smog because they can cause the conversion from NO to NO₂, and the latter is the immediate precursor to ozone smog and a major driving force in urban air pollution.¹³ Alkyl peroxyl radicals also play a key role in the heterogeneous oxidation of hydrocarbons.¹⁴ As chain carriers by abstracting hydrogen atoms from other organic molecules or by simply one-electron-oxidizing them in degradation of organic materials in the presence of oxygen, they are also believed to have relations with the aging process of many high molecular weight polymers, such as rubber and plastic.¹⁵ Furthermore, alkyl peroxyl radicals play an important role in the process of lipid autoxidation and nucleic acid damage, which has been considered to have many deleterious effects on membrane structure and cellular function responsible for various diseases and aging.^{11,12}

The electron affinity (EA) is both a key spectroscopic value and vitally important for use in the chemical cycle to determine bond dissociation energy. However, until recent years, there have been few experimental or theoretical studies for the EA of the above radicals.^{13,16} The thermochemical properties and the ground or electronic states of the neutral and anion species are indispensable tools for understanding chemical reactivity and predicting the reaction mechanism. With this motivation, we have carried out a detailed study of structures, thermochemistry, and electron affinities of the above radicals and their anions using density functional theory (DFT).^{17–19}

When predicting molecular energies, structures, and electron affinities, there are many theoretical approaches, but considering both reliability and computational expense, the GGA density functional theory is effective for predicting electron affinities

of many organic species.^{20–22} The theoretical prediction of electron affinities has historically been generally difficult due to the desired result's being a small difference between two large energies; but recent work has shown that some carefully chosen DFT methods are dependable for EA predictions. Although, for DFT calculations of anions, there are some problems (such as the unphysical asymptotic behavior of all their functionals and the lack of a complete basis set limit of some anions^{23,24}) DFT is, indeed, applicable to anions and provides EA predictions within experimental error and achieves satisfying results. For a general discussion of the reliability of DFT studies, the reader is referred to the 2002 review of Rienstra-Kiracofe et al.²² They suggested that B3PW91 and BPW91 methods might outperform the B3LYP, BLYP, and BP86 functionals.

The object of the present study is to systematically apply seven contemporary forms of density functional theory to determine the electron affinities and other properties of the R-OO/R-OO⁻ (R = CH₃, C₂H₅, *n*-C₃H₇, *n*-C₄H₉, *n*-C₅H₁₁, *i*-C₃H₇, *t*-C₄H₉). Our specific interest is (a) the comparison of the theoretical electron affinities with available experimental results; (b) the relationship between the neutral R-OO species and their anions; (c) the predictions of other properties, including vibrational frequencies; and (d) the comparison of the different DFT methods. In our paper, the experimental electron affinities are adiabatic (EA_{ad}), which are available on the internet as part of the NIST Chemistry Webbook.²⁵ We would like to establish reliable theoretical predictions for these R-OO species in the absence of experimental results and in some cases to challenge existing experiments.

Theoretical Methods

The seven pure DFT or hybrid Hartree–Fock/DFT methods used in our study are (a) Becke's 1988 exchange functional²⁶ with Lee, Yang, and Parr's correlation functional²⁷ (BLYP); (b) the half-and-half exchange functional²⁸ with the LYP correlation functional (B3LYP); (c) Becke's three-parameter hybrid functional²⁹ with the LYP correlation functional (BPW91); (d)

* To whom correspondence should be addressed.

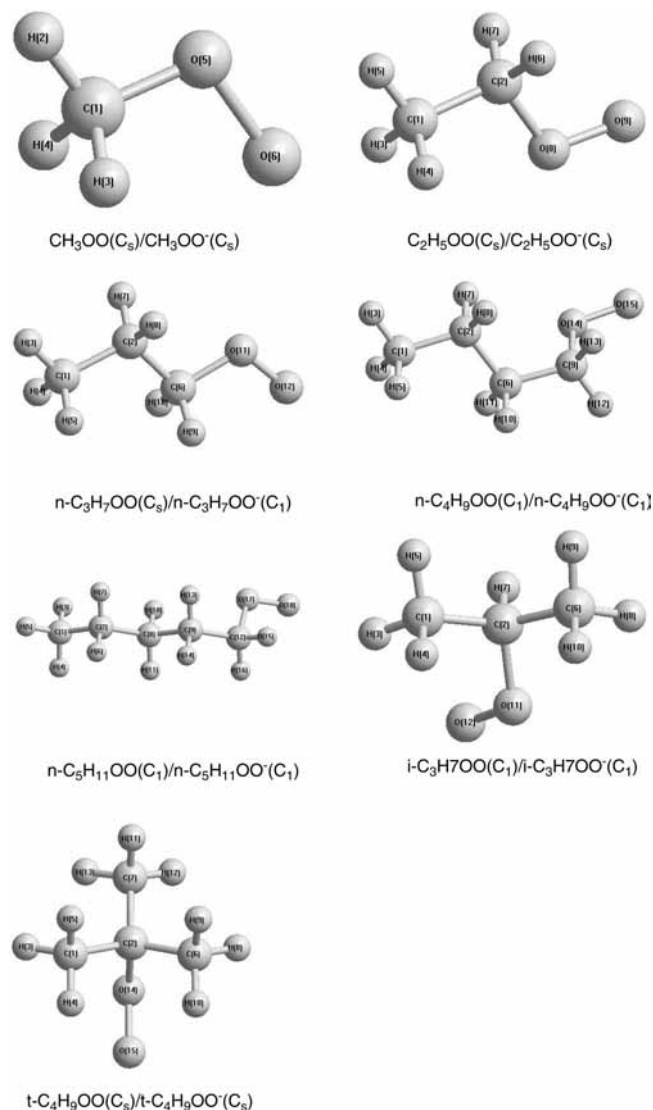


Figure 1. Optimized geometries for R-OO/R-OO⁻ (R = CH₃, C₂H₅, n-C₃H₇, n-C₄H₉, n-C₅H₁₁, i-C₃H₇, and t-C₄H₉).

Becke's 1988 exchange functional with Perdew's correlation functional³⁰ (BP86); (e) Becke's three-parameter hybrid functional with Perdew's correlation functional (B3P86); (f) Becke's three-parameter hybrid functional with Perdew and Wang's 1991 gradient-corrected correlation functional³¹ (B3PW91); and (g) Becke's 1988 exchange functional with Perdew and Wang's 1991 gradient-corrected correlation functional (BPW91). For the two simplest species, CH₃OO and C₂H₅OO, we also applied MP2 methods to compare with the seven pure DFT or hybrid Hartree–Fock/DFT methods above.

Restricted methods were used for all closed-shell systems, and unrestricted methods were employed for the open-shell species. All the electron affinities and molecular structures have been determined using the Gaussian 98 program suite.³² The default numerical integration grid (75 302) of Gaussian 98 was initially applied.

The standard double- ζ plus polarization (DZP) basis sets are constructed from the Huzinaga–Dunning–Hay^{33–36} sets of contracted Gaussian functions by adding a set of five pure d-type polarization functions for C, O, and a p-type polarization functions for H [$\alpha_p(\text{H}) = 0.75$, $\alpha_d(\text{C}) = 0.75$, $\alpha_d(\text{O}) = 0.85$]. Since diffuse functions are important for the anions, the DZP basis was augmented with diffuse functions; each heavy atom received one

TABLE 1: Adiabatic and Vertical Electron Affinities of the Neutral C_nH_{2n+1}OO and Vertical Detachment Energies of Their Anions in Electronvolts^a

compd	method	EAad	corrected EAad	VDE	
CH ₃ OO	B3LYP	1.046	1.099	1.469	
	BLYP	1.015	1.067	1.373	
	BHLYP	0.741	0.794	1.206	
	B3PW91	0.906	0.960	1.330	
	BPW91	0.938	0.993	1.304	
	B3P86	1.489	1.543	1.915	
	BP86	1.096	1.150	1.456	
	MP2	1.105	1.154	1.842	
	exptl	1.161 ± 0.005 ^b			
	C ₂ H ₅ OO	B3LYP	1.027	1.084	1.483
BLYP		0.981	1.038	1.379	
BHLYP		0.732	0.790	1.221	
B3PW91		0.886	0.944	1.339	
BPW91		0.905	0.964	1.303	
B3P86		1.472	1.530	1.925	
BP86		1.065	1.124	1.458	
MP2		1.110	1.164	1.880	
exptl		1.186 ± 0.004 ^b			
n-C ₃ H ₇ OO		B3LYP	1.043	1.103	1.504
	BLYP	0.993	1.054	1.388	
	BHLYP	0.752	0.812	1.250	
	B3PW91	0.902	0.964	1.365	
	BPW91	0.918	0.980	1.328	
	B3P86	1.493	1.554	1.953	
	BP86	1.084	1.146	1.480	
	exptl				
	n-C ₄ H ₉ OO	B3LYP	1.061	1.123	1.518
		BLYP	1.026	1.086	1.386
BHLYP		0.768	0.831	1.267	
B3PW91		0.922	0.985	1.377	
BPW91		0.945	1.009	1.324	
B3P86		1.511	1.574	1.966	
BP86		1.109	1.173	1.487	
exptl					
n-C ₅ H ₁₁ OO		B3LYP	1.067	1.129	1.526
		BLYP	1.038	1.098	1.385
	BHLYP	0.774	0.837	1.276	
	B3PW91	0.928	0.992	1.385	
	BPW91	0.955	1.020	1.321	
	B3P86	1.517	1.581	1.975	
	BP86	1.117	1.184	1.486	
	exptl				
	i-C ₃ H ₇ OO	B3LYP	1.032	1.095	1.514
		BLYP	0.984	1.045	1.394
BHLYP		0.742	0.805	1.257	
B3PW91		0.895	0.960	1.375	
BPW91		0.912	0.978	1.331	
B3P86		1.487	1.552	1.970	
BP86		1.079	1.145	1.493	
exptl					
t-C ₄ H ₉ OO		B3LYP	0.998	1.067	1.513
		BLYP	0.931	0.998	1.400
	BHLYP	0.722	0.791	1.257	
	B3PW91	0.870	0.941	1.386	
	BPW91	0.873	0.945	1.351	
	B3P86	1.466	1.537	1.983	
	BP86	1.043	1.114	1.517	
	exptl	1.196 ± 0.011 ^c			

^a Values are corrected for ZPVE and were obtained with the DZP++ basis set. ^b See ref 13. ^c See ref 68.

additional s-type and one set of p-type functions, and the H atom received one s-diffuse function. The diffuse function orbital exponents were determined in an “even-tempered sense” as a mathematical extension of the primitive set according to the prescription of Lee and Schaefer.³⁷ [$\alpha_s(\text{C}) = 0.0430$, $\alpha_p(\text{C}) = 0.0363$, $\alpha_s(\text{H}) = 0.04415$, $\alpha_s(\text{O}) = 0.0823$, $\alpha_p(\text{O}) = 0.0651$]. The

TABLE 2: Optimized Geometry for the CH₃OO and the Corresponding Anion CH₃OO⁻ ^a

	B3LYP	BLYP	BHLYP	B3PW91	BPW91	B3P86	BP86	MP2
CH ₃ OO 2-A''								
R (1, 5)	1.453	1.477	1.430	1.445	1.465	1.442	1.465	1.456
R (5, 6)	1.325	1.353	1.301	1.314	1.337	1.313	1.339	1.314
A (1, 5, 6)	111.2	111.1	111.3	111.3	111.2	111.2	111.0	110.5
CH ₃ OO ⁻								
R (1, 5)	1.389	1.408	1.372	1.382	1.397	1.380	1.398	1.397
R (5, 6)	1.478	1.506	1.452	1.462	1.484	1.460	1.485	1.480
A (1, 5, 6)	106.4	106.3	106.6	106.3	106.1	106.1	106.0	104.7

^a All bond distances are in angstroms, all bond angles are in degrees, and all results were obtained with the DZP++ basis set.

TABLE 3: Harmonic frequencies (ω/cm^{-1}) for the CH₃OO and the Corresponding Anion CH₃OO⁻

		B3LYP	BLYP	BHLYP	B3PW91	BPW91	B3P86	BP86	MP2	expl ^{a, b, c}
CH ₃ OO										
<i>a'</i>	ω_1	3169	3086	3266	3188	3113	3192	3095	3264	3032
	ω_2	3057	2976	3153	3068	2995	3072	2978	3125	2954
	ω_3	1473	1427	1537	1472	1427	1472	1420	1513	1448
	ω_4	1435	1381	1504	1433	1381	1433	1374	1470	1410
	ω_5	1222	1150	1313	1246	1167	1251	1162	1275	1180
	ω_6	1158	1064	1237	1172	1100	1174	1097	1201	1109
	ω_7	919	832	1005	939	861	945	860	954	902
	ω_8	486	460	513	491	467	492	466	498	492
<i>a''</i>	ω_9	3156	3074	3252	3172	3099	3176	3081	3255	3024
	ω_{10}	1462	1415	1523	1460	1416	1460	1408	1497	1434
	ω_{11}	1116	1065	1182	1116	1067	1117	1063	1143	na
	ω_{12}	134	131	143	136	133	135	132	123	na
CH ₃ OO ⁻										
<i>a'</i>	ω_1	2936	2838	3044	2953	2861	2958	2844	3069	
	ω_2	2873	2777	2988	2880	2790	2885	2773	2974	
	ω_3	1485	1442	1545	1483	1441	1483	1433	1517	
	ω_4	1412	1363	1478	1408	1360	1408	1352	1432	
	ω_5	1192	1143	1253	1201	1155	1204	1150	1205	
	ω_6	1081	997	1170	1100	1027	1104	1023	1108	
	ω_7	820	758	885	849	794	855	794	871	
	ω_8	423	401	447	426	405	428	406	436	
<i>a''</i>	ω_9	2885	2775	3012	2895	2787	2900	2769	3043	
	ω_{10}	1409	1356	1478	1403	1351	1402	1341	1442	
	ω_{11}	1144	1103	1197	1144	1105	1146	1100	1156	
	ω_{12}	272	264	276	277	272	280	273	278	

^a See ref 13. ^b See ref 14. ^c See ref 46.

TABLE 4: Optimized Geometry for the C₂H₅OO and the Corresponding Anion C₂H₅OO⁻ ^a

	B3LYP	BLYP	BHLYP	B3PW91	BPW91	B3P86	BP86	MP2
C ₂ H ₅ OO								
R (1, 2)	1.520	1.530	1.510	1.514	1.522	1.512	1.523	1.514
R (2, 8)	1.466	1.493	1.441	1.458	1.481	1.455	1.481	1.467
R (8, 9)	1.324	1.352	1.301	1.314	1.336	1.313	1.338	1.314
A (1, 2, 8)	107.5	107.4	107.5	107.6	107.6	107.6	107.5	106.8
A (2, 8, 9)	111.6	111.5	111.6	111.6	111.6	111.5	111.4	110.9
C ₂ H ₅ OO ⁻								
R (1, 2)	1.537	1.551	1.525	1.532	1.542	1.529	1.543	1.529
R (2, 8)	1.389	1.406	1.373	1.383	1.397	1.381	1.398	1.397
R (8, 9)	1.481	1.511	1.454	1.464	1.488	1.462	1.489	1.483
A (1, 2, 8)	109.3	109.0	109.5	109.3	109.1	109.3	109.0	108.4
A (2, 8, 9)	107.1	107.0	107.2	107.0	106.9	106.8	106.8	105.5

^a All bond distances are in angstroms, all bond angles are in degrees, and all results were obtained with the DZP++ basis set.

final basis sets are, thus, H (5s1p/3s1p); C, O (10s6p1d/5s3p1d). This extended basis will be denoted as "DZP++".

All R-OO stationary point geometries were interrogated by the evaluation of their harmonic vibrational frequencies at each of the seven different levels of theory. Zero-point vibrational energies (ZPVEs) were evaluated at the seven levels (Table 1 of the Supporting Information). The differ-

ences may be used as corrections to the adiabatic electron affinities. The total energy of seven radicals and the ZPVE corrected total energy are displayed in Table 2 of the Supporting Information.

The electron affinities are evaluated as the difference of total energies in the following manner: the adiabatic electron affinity is determined as EA_{ad} = $E(\text{optimized neutral}) - E(\text{optimized$

TABLE 5: Harmonic frequencies(ω/cm^{-1}) for the $\text{C}_2\text{H}_5\text{OO}$ and the Corresponding Anion $\text{C}_2\text{H}_5\text{OO}^-$

		B3LYP	BLYP	BHLYP	B3PW91	BPW91	B3P86	BP86	MP2	exptl ^{a, b, c}
$\text{C}_2\text{H}_5\text{OO}$										
a'	ω_1	3130	3047	3223	3154	3082	3158	3064	3218	
	ω_2	3068	2987	3166	3080	3007	3083	2989	3140	2964
	ω_3	3053	2976	3142	3067	3000	3071	2984	3111	2988
	ω_4	1500	1459	1561	1496	1457	1497	1450	1529	1448, 1451
	ω_5	1486	1439	1546	1484	1438	1484	1431	1521	1474
	ω_6	1415	1370	1479	1413	1368	1414	1361	1447	1380
	ω_7	1368	1317	1431	1364	1317	1364	1310	1396	1283
	ω_8	1210	1109	1311	1244	1147	1250	1143	1276	1173
	ω_9	1130	1075	1189	1137	1094	1139	1090	1160	1070, 1112
	ω_{10}	1021	963	1088	1037	983	1042	980	1063	880, 1009
	ω_{11}	842	772	906	853	793	856	791	870	800
	ω_{12}	498	469	527	504	478	506	478	510	499
	a''	ω_{13}	305	290	321	305	291	306	290	312
ω_{14}		3142	3061	3237	3162	3092	3166	3074	3231	2999, 3016
ω_{15}		3120	3038	3215	3137	3063	3140	3044	3212	2988
ω_{16}		1477	1439	1531	1474	1437	1474	1430	1503	1397
ω_{17}		1265	1220	1324	1266	1223	1266	1217	1289	
ω_{18}		1139	1091	1199	1137	1091	1138	1087	1165	1110
ω_{19}		798	773	831	797	773	796	769	822	838
ω_{20}		224	212	239	225	214	225	213	236	
ω_{21}		76	72	84	78	74	77	73	64	
$\text{C}_2\text{H}_5\text{OO}^-$										
a'	ω_1	3070	2990	3161	3095	3026	3100	3008	3165	
	ω_2	3004	2927	3094	3020	2952	3100	2935	3069	
	ω_3	2880	2782	2996	2888	2797	2893	2779	2988	
	ω_4	1507	1463	1567	1503	1461	1504	1454	1530	
	ω_5	1486	1444	1542	1483	1443	1483	1435	1513	
	ω_6	1370	1323	1436	1367	1320	1368	1313	1403	
	ω_7	1341	1295	1402	1334	1289	1334	1282	1356	
	ω_8	1190	1127	1261	1208	1151	1213	1148	1205	
	ω_9	1049	988	1113	1060	1008	1064	1006	1087	
	ω_{10}	913	858	974	930	876	935	875	954	
	ω_{11}	824	769	878	839	794	842	791	854	
	ω_{12}	462	440	483	466	448	468	448	474	
	a''	ω_{13}	288	273	304	289	274	290	274	296
ω_{14}		3082	2999	3176	3105	3033	3109	3015	3182	
ω_{15}		2875	2765	3002	2885	2777	2889	2758	3024	
ω_{16}		1459	1417	1515	1455	1415	1454	1407	1485	
ω_{17}		1223	1176	1282	1219	1174	1219	1167	1240	
ω_{18}		1168	1126	1220	1167	1128	1169	1124	1186	
ω_{19}		797	768	828	795	769	794	763	819	
ω_{20}		232	217	248	230	215	230	214	238	
ω_{21}		127	111	135	130	119	132	119	126	

^a See ref 13. ^b See ref 58. ^c See ref 59.

anion), and the vertical detachment energy of the anion, as $\text{VDE} = E(\text{neutral at optimized anion geometry}) - E(\text{optimized anion})$.

Results and Discussion

A. CH_3OO and CH_3OO^- . There are numerous previous studies on the methylperoxy radical both in experiment and theory^{1,2,6,13,14,38-50} because of its important role in atmospheric and internal combustion chemistry, most of them related to UV absorption spectrum and kinetics. In 1973, Parkes et al. first studied the UV absorption spectra of CH_3OO and their mutual reaction.³⁸ In 2001, Blanksby, Ramond, et al. studied its negative ion photoelectron spectroscopy and gave the adiabatic electron affinity.¹³ The following year, Nandi, Blanksby, et al. determined the fundamental infrared bands of CH_3OO and computed the harmonic frequencies by the UB3LYP/6-311G(d,p) method.¹⁴

The equilibrium geometries of the ground states of CH_3OO and CH_3OO^- are displayed in Figure 1, and geometric parameters are in Table 2. Our DFT and MP2 results show a C_s symmetry with a ${}^2A''$ state for the ground state of CH_3OO . This

result is consistent with the previous results of Nandi, Blanksby, et al.¹⁴ The bond lengths of C–O and O–O are in the range of 1.430–1.477 and 1.301–1.353 Å, respectively. The BHLYP method gets the shortest bond length, and the BLYP gets the longest. The bond angle values of C–O–O range from 111.0° to 111.3°.

The anion CH_3OO^- also has C_s symmetry with the state of ${}^1A'$. The bond lengths of C–O and O–O are in the range of 1.372–1.408 and 1.452–1.506 Å, respectively. The bond angle of C–O–O ranges from 106.0° to 106.6°. It is noticeable that both bond lengths and bond angles between the neutral radical and anion have changed dramatically. The C–O bond gets shorter; quite the reverse, the O–O gets longer from radical to anion and the bond angle value of C–O–O decreases by about 4.7–5.1°. In addition, the optimized geometries for the seven DFT methods vary only slightly among each other.

The theoretical EAad and VDE, as well as the experimental electron affinity data, are listed in Table 1. The range of EAad corrected is predicted to be 0.794–1.543 eV with the seven DFT methods. The BHLYP method predicts the smallest EAad

TABLE 6: Optimized Geometry for the $n\text{-C}_3\text{H}_7\text{OO}$ and the Corresponding Anion $n\text{-C}_3\text{H}_7\text{OO}^-$ ^a

	B3LYP	BLYP	BHLYP	B3PW91	BPW91	B3P86	BP86
$n\text{-C}_3\text{H}_7\text{OO}$							
$R(1, 2)$	1.536	1.549	1.524	1.530	1.540	1.528	1.541
$R(2, 6)$	1.523	1.534	1.512	1.518	1.526	1.515	1.527
$R(6, 11)$	1.464	1.492	1.440	1.456	1.479	1.453	1.479
$R(11, 12)$	1.325	1.352	1.301	1.314	1.336	1.313	1.339
$A(1, 2, 6)$	111.4	111.4	111.3	111.4	111.4	111.2	111.3
$A(2, 6, 11)$	107.8	107.7	107.8	107.9	107.9	107.9	107.8
$A(6, 11, 12)$	111.7	111.6	111.7	111.7	111.6	111.6	111.5
$D(1, 2, 6, 11)$	180.0	180.0	180.0	180.0	180.0	180.0	180.0
$D(2, 6, 11, 12)$	180.0	180.0	180.0	180.0	180.0	180.0	180.0
$n\text{-C}_3\text{H}_7\text{OO}^-$							
$R(1, 2)$	1.537	1.549	1.525	1.531	1.540	1.528	1.541
$R(2, 6)$	1.539	1.552	1.527	1.534	1.544	1.531	1.545
$R(6, 11)$	1.389	1.406	1.373	1.382	1.397	1.381	1.397
$R(11, 12)$	1.481	1.510	1.454	1.465	1.487	1.463	1.488
$A(1, 2, 6)$	113.2	113.5	112.9	113.1	113.4	112.8	113.1
$A(2, 6, 11)$	109.6	109.4	109.8	109.7	109.5	109.6	109.4
$A(6, 11, 12)$	107.3	107.3	107.4	107.1	107.1	107.0	107.1
$D(1, 2, 6, 11)$	61.8	62.0	61.5	61.7	61.8	61.3	61.3
$D(2, 6, 11, 12)$	179.8	179.5	-179.7	-179.9	179.9	-180.0	179.5

^a All bond distances are in angstroms, all bond angles are in degrees, and all results were obtained with the DZP++ basis set.

(0.794 eV), and the B3P86 method predicts the largest value (1.543 eV). The result of BP86 (1.150 eV) matches the experimental values (1.161 ± 0.005 eV) obtained by Blanksby, Ramond, et al. very well (only deviating by about 0.011 eV). It also matches the MP2 result (1.154 eV) very well. B3LYP (1.099 eV), BLYP (1.067 eV) results are also reasonable. From the above results, we can see that the application of the employed DFT methods to ROO species is available. The theoretical vertical detachment energy VDE is 1.456 eV.

The harmonic frequencies obtained by seven DFT methods present in Table 3. (All the frequencies obtained in this study are not scaled by any scale factor.) Nandi, Blanksby, et al. give the experimental vibrational frequencies and the UB3LYP/6-311G(p,d) harmonic frequencies.¹⁴ To compare with the experimental frequencies data of Nandi, Blanksby, et al. and Ase, Bock, et al.,^{14,46} we find our theoretical frequencies agree well with experimental assigned values. Among the seven functionals, three pure DFT functionals (BLYP, BPW91, and BP86) predict values slightly below or near the experimental values, whereas the others consistently overestimate values. The seven methods can be ranked by total percent deviation from experiment: BPW91 (0.98%), BP86 (1.41%), BLYP (2.15%), B3LYP (2.65%), B3PW91 (3.42%), B3P86 (3.60%), and BHLYP (7.95%). It can be seen that our theoretical results are quite good except for BHLYP. The three pure DFT methods give better predictions and could often be used without scaling. Our results are also consistent with previous studies by Scott and Radom,⁵¹ Brown et al.,⁵² and Wenguo Xu et al.²⁰

B. $\text{C}_2\text{H}_5\text{OO}$ and $\text{C}_2\text{H}_5\text{OO}^-$. The ethyl peroxy radical $\text{C}_2\text{H}_5\text{OO}$ is also a significant intermediate in many chemical processes. Numerous articles in the literature have reported both experiment and theory.^{13,43,44,47,48,53-59} Recent negative ion photoelectron spectroscopy studies of $\text{C}_2\text{H}_5\text{OO}$ measured the adiabatic electron affinity of the ground state to be 1.186 ± 0.004 eV,¹³ and the vibrational frequencies also have been reported, as well.^{13,58,59}

The optimized geometries of the ground state of $\text{C}_2\text{H}_5\text{OO}$ and $\text{C}_2\text{H}_5\text{OO}^-$ are provided in Figure 1 and Table 4. All functionals predict a C_s symmetry with a ${}^2A''$ ground state for $\text{C}_2\text{H}_5\text{OO}$ and a C_s symmetry with a ${}^1A'$ ground state for $\text{C}_2\text{H}_5\text{OO}^-$. For the radical, the range of the bond lengths of C—O

and O—O are from 1.441 to 1.493 Å and from 1.301 to 1.352 Å. In the same way as the results for the CH_3OO species, the BHLYP gives the shortest bond length and the BLYP the longest. The bond angle values of C—O—O from seven functionals are predicted to be 111.4–111.6°, with very slight variation to each other. For the anion $\text{C}_2\text{H}_5\text{OO}^-$, the same bond lengths and bond angle are in the range of 1.373–1.406 Å, 1.454–1.511 Å, and 111.0–111.3°, respectively. Just as the trend in CH_3OO and CH_3OO^- , the bond length values of C—O from all the functionals in anion are shorter than those in radical. On the contrary, the O—O bond gets longer. Like CH_3OO and CH_3OO^- , the bond angle C—O—O decreases about 4.4–4.7° when an electron is attached to the radical.

Our theoretical neutral anion energy separations for the $\text{C}_2\text{H}_5\text{OO}$ and $\text{C}_2\text{H}_5\text{OO}^-$, as well as experimental electron affinity data, are shown in Table 1. The adiabatic electron affinity EAad is predicted to be 0.790–1.530 eV. Compared with the experimental value (1.186 ± 0.005 eV),¹³ the present DZP++ BP86 EAad value provides the most favorable comparison with the experimental result, of which the absolute error is only 0.062 eV. The B3LYP (1.084 eV) and BLYP (1.038 eV) methods are also considered to be the acceptable ones. The range of VDE is from 1.221 to 1.925 eV.

Our harmonic vibrational frequencies derived from the seven DFT methods for $\text{C}_2\text{H}_5\text{OO}$ and $\text{C}_2\text{H}_5\text{OO}^-$ are displayed in Table 5. Chettur and Snelson observed a number of bands ascribed to $\text{C}_2\text{H}_5\text{OO}$ in Ar matrix data in 1987.⁵⁸ Mah, Cabrera, et al. measured the midinfrared spectrum of the gas-phase ethyl peroxy radical in 2003.⁵⁹ Blanksby, Ramond, et al. derived the O—O stretch frequency in 2001.¹³ We have compared our theoretical frequencies with the experimental data of Chettur and Snelson; Mah, Cabrera, et al.; and Blanksby, Ramond, et al. Excellent agreement of most results (except the C—C stretching mode (880 cm^{-1}) frequency of Mah, Cabrera, et al.) was found. Our prediction shows 9.4–23.6% deviation from the data of Mah, Cabrera, et al., but only 1.2–7.8% deviation from that of Chettur and Snelson. So maybe the latter experimental data is more reliable. The same consequence occurs on the O—O stretch frequency. Our results have the best agreement with the data of Chettur and Snelson. We also find that the BHLYP once again show the poorest agreement (7.7%).

TABLE 7: Harmonic Frequencies (ω/cm^{-1}) for the $n\text{-C}_3\text{H}_7\text{OO}$ and the Corresponding Anion $n\text{-C}_3\text{H}_7\text{OO}^-$

		B3LYP	BLYP	BHLYP	B3PW91	BPW91	B3P86	BP86	exptl
$n\text{-C}_3\text{H}_7\text{OO}$									
a'	ω_1	3119	3037	3211	3141	3071	3146	3054	
	ω_2	3060	2980	3157	3073	3001	3075	2983	
	ω_3	3049	2969	3144	3065	2994	3068	2975	
	ω_4	3037	2961	3126	3051	2985	3055	2968	
	ω_5	1508	1468	1564	1503	1464	1504	1458	
	ω_6	1490	1450	1553	1487	1448	1487	1441	
	ω_7	1485	1438	1542	1483	1437	1483	1429	
	ω_8	1413	1372	1475	1409	1369	1410	1362	
	ω_9	1401	1345	1468	1402	1349	1402	1343	
	ω_{10}	1319	1276	1377	1315	1273	1315	1267	
	ω_{11}	1208	1111	1311	1242	1143	1248	1140	
	ω_{12}	1145	1087	1197	1152	1112	1154	1108	
	ω_{13}	1051	1006	1100	1066	1029	1069	1025	
	ω_{14}	947	890	1038	970	901	977	899	
	ω_{15}	917	849	954	922	878	923	877	
	ω_{16}	486	460	512	490	467	491	466	
	ω_{17}	395	375	416	397	378	398	378	
	ω_{18}	198	189	208	198	189	197	188	
a''	ω_{19}	3125	3043	3222	3141	3069	3144	3050	
	ω_{20}	3107	3026	3200	3128	3057	3131	3037	
	ω_{21}	3085	3003	3180	3106	3034	3109	3015	
	ω_{22}	1495	1456	1548	1491	1455	1491	1447	
	ω_{23}	1306	1268	1357	1305	1269	1305	1262	
	ω_{24}	1243	1200	1299	1242	1201	1242	1195	
	ω_{25}	1150	1102	1209	1148	1104	1149	1099	
	ω_{26}	882	855	917	881	856	880	850	
	ω_{27}	759	738	786	757	737	757	734	
	ω_{28}	231	224	239	233	227	233	226	
	ω_{29}	108	100	117	109	102	109	100	
	ω_{30}	66	61	73	67	63	67	63	
$n\text{-C}_3\text{H}_7\text{OO}^-$									
a	ω_1	3116	3034	3211	3136	3065	3140	3047	
	ω_2	3063	2979	3155	3087	3015	3091	2996	
	ω_3	3034	2951	3129	3057	2985	3061	2966	
	ω_4	3006	2925	3099	3023	2952	3026	2934	
	ω_5	2992	2912	3083	3011	2941	3015	2923	
	ω_6	2878	2775	3002	2887	2789	2893	2773	
	ω_7	2860	2753	2983	2871	2768	2873	2746	
	ω_8	1498	1458	1560	1495	1455	1495	1447	
	ω_9	1496	1451	1552	1493	1450	1493	1442	
	ω_{10}	1473	1434	1528	1469	1432	1469	1423	
	ω_{11}	1461	1419	1519	1457	1416	1457	1408	
	ω_{12}	1387	1346	1446	1382	1342	1383	1335	
	ω_{13}	1355	1303	1426	1356	1305	1357	1298	
	ω_{14}	1340	1297	1400	1334	1290	1333	1283	
	ω_{15}	1285	1245	1337	1286	1248	1286	1242	
	ω_{16}	1212	1166	1270	1210	1166	1210	1160	
	ω_{17}	1182	1127	1250	1195	1142	1199	1138	
	ω_{18}	1155	1110	1209	1157	1117	1158	1112	
	ω_{19}	1080	1027	1137	1092	1049	1096	1046	
	ω_{20}	988	943	1039	995	954	997	950	
	ω_{21}	912	881	951	911	881	911	876	
	ω_{22}	872	834	932	890	848	895	846	
	ω_{23}	866	804	910	879	833	883	833	
	ω_{24}	747	716	780	746	719	747	716	
	ω_{25}	494	472	517	498	478	499	477	
	ω_{26}	349	333	366	350	335	352	336	
	ω_{27}	290	278	304	290	278	291	278	
	ω_{28}	191	185	201	191	184	191	185	
	ω_{29}	130	124	138	130	124	131	125	
	ω_{30}	100	83	107	103	92	104	93	

C. $n\text{-C}_3\text{H}_7\text{OO}$ and $n\text{-C}_3\text{H}_7\text{OO}^-$. Adachi and Basco studied the spectra of n -propyl peroxy radicals and rate constants for mutual interaction via flash photolysis technique in 1982.⁶⁰ Until 2005, observation of the cavity ringdown spectra of $n\text{-C}_3\text{H}_7\text{OO}$ and conformational analysis had been done by Zalyubovsky, Tarczay, et al.^{61,62} As the first member of the alkyl peroxy

family for which it is possible to form a low-energy, six-membered ring transition state, $n\text{-C}_3\text{H}_7\text{OO}$ has recently been proposed as a model system for $\text{RO}_2 \leftrightarrow \text{QOOH}$ isomerization.⁶³

The ground state structures of $n\text{-C}_3\text{H}_7\text{OO}$ and $n\text{-C}_3\text{H}_7\text{OO}^-$ are shown in Figure 1, and the structural parameters are provided in Table 6. For the $n\text{-C}_3\text{H}_7\text{OO}$, the structure of the ground state

TABLE 8: Optimized Geometry for the $n\text{-C}_4\text{H}_9\text{OO}$ and the Corresponding Anion $n\text{-C}_4\text{H}_9\text{OO}^-$ ^a

	B3LYP	BLYP	BHLYP	B3PW91	BPW91	B3P86	BP86
$n\text{-C}_4\text{H}_9\text{OO}$							
$R(1, 2)$	1.534	1.547	1.523	1.529	1.538	1.526	1.539
$R(2, 6)$	1.537	1.549	1.525	1.531	1.541	1.529	1.542
$R(6, 9)$	1.523	1.533	1.512	1.518	1.526	1.515	1.527
$R(9, 14)$	1.467	1.495	1.442	1.458	1.482	1.456	1.482
$R(14, 15)$	1.324	1.352	1.301	1.314	1.336	1.313	1.338
$A(1, 2, 6)$	112.6	112.7	112.4	112.6	112.7	112.5	112.6
$A(2, 6, 9)$	114.1	114.3	113.9	114.2	114.4	114.0	114.2
$A(6, 9, 14)$	107.9	107.8	107.9	108.1	108.1	107.9	107.9
$A(9, 14, 15)$	111.7	111.6	111.7	111.7	111.7	111.6	111.6
$D(1, 2, 6, 9)$	-179.6	-179.5	-179.6	-179.6	-179.5	-179.7	-179.7
$D(2, 6, 9, 14)$	-67.0	-68.0	-66.0	-67.0	-67.9	-66.6	-67.6
$D(6, 9, 14, 15)$	177.5	177.5	177.6	176.9	176.8	176.9	176.8
$n\text{-C}_4\text{H}_9\text{OO}^-$							
$R(1, 2)$	1.536	1.549	1.525	1.530	1.540	1.528	1.541
$R(2, 6)$	1.535	1.548	1.524	1.530	1.540	1.527	1.540
$R(6, 9)$	1.539	1.551	1.526	1.533	1.544	1.530	1.544
$R(9, 14)$	1.389	1.411	1.373	1.383	1.399	1.381	1.399
$R(14, 15)$	1.480	1.500	1.454	1.464	1.482	1.462	1.484
$A(1, 2, 6)$	113.5	113.6	113.3	113.5	113.7	113.4	113.5
$A(2, 6, 9)$	113.5	113.6	113.3	113.4	113.5	113.2	113.2
$A(6, 9, 14)$	109.6	109.4	109.7	109.6	109.5	109.5	109.3
$A(9, 14, 15)$	107.2	107.5	107.3	107.1	107.2	107.0	107.1
$D(1, 2, 6, 9)$	-179.9	-177.4	179.3	179.8	-178.1	179.8	-178.1
$D(2, 6, 9, 14)$	-61.0	-59.8	-61.1	-60.9	-59.8	-60.4	-59.3
$D(6, 9, 14, 15)$	-178.7	-174.7	-179.7	-179.2	-176.4	-179.1	-176.3

^a All bond distances are in angstroms, all bond angles are in degrees, and all results were obtained with the DZP++ basis set.

displays a C_s symmetry with an $^2A''$ electronic state derived from all seven DFT methods. No experimental or theoretical data are available for comparison. Our DFT methods predict the bond lengths of the C–O and O–O bonds to be 1.440–1.492 and 1.301–1.352 Å, which is very similar to their counterparts in C_2H_5OO (1.441–1.493 and 1.30–1.352 Å). The bond angle for C–O–O is in the range from 111.4° to 111.6°, just like that in C_2H_5OO (111.4–111.6°). For the structure of the ground state of the anion $n\text{-C}_3\text{H}_7\text{OO}^-$, we get two stable structures, one showing C_1 symmetry, and the other, C_s symmetry. All seven DFT results show that C_1 symmetry is more stable in energy by about 0.01–0.015 eV than C_s symmetry. That is, the C_s symmetry structure is a local minimal point on the potential energy surface. Again, we find the same trend that the C–O bond length decreases to 1.373–1.406 Å and the O–O increases to 1.454–1.510 Å.

The theoretical EAad and VDE are listed in Table 1. The range of EAad is from 0.812 to 1.554 eV via the seven functionals. The VDE value is in the range from 1.250 to 1.953 eV. No experimental or theoretical data are available for comparison.

The theoretical harmonic frequencies for $n\text{-C}_3\text{H}_7\text{OO}$ and $n\text{-C}_3\text{H}_7\text{OO}^-$ are shown in Table 7. As usual, the BHLYP method gets the largest values, and the B3LYP method predicts the smallest. The values obtained via BLYP, BPW91, and BP86 are similar to each other, as are the values of B3LYP, B3PW91, and B3P86. The calculated O–O stretching frequencies by the seven methods are B3LYP (1208 cm^{-1}), BLYP (1111 cm^{-1}), BHLYP (1311 cm^{-1}), B3PW91 (1242 cm^{-1}), BPW91 (1143 cm^{-1}), B3P86 (1248 cm^{-1}), and BP86 (1140 cm^{-1}). No experimental data can be found for comparison.

D. $n\text{-C}_4\text{H}_9\text{OO}$ and $n\text{-C}_4\text{H}_9\text{OO}^-$. The optimized geometry of the ground state of $n\text{-C}_4\text{H}_9\text{OO}$ and $n\text{-C}_4\text{H}_9\text{OO}^-$ is given in Figure 1 and Table 8. All the DFT methods predict the neutral species and anion to be C_1 symmetry zigzag structure. The general trend of the bond lengths is BLYP > BP86 ~ BPW91

> B3LYP > B3PW91 ~ B3P86 > BHLYP. For the neutral species $n\text{-C}_4\text{H}_9\text{OO}$, the bond distances of C–O and O–O are in a range of 1.442–1.495 and 1.301–1.352 Å, respectively. They are also very close to their counterparts in C_2H_5OO and $n\text{-C}_3H_7OO$. For the anion $n\text{-C}_4H_9OO^-$, the C–O bond lengths range from 1.373 to 1.411 Å, and the O–O bond lengths, from 1.454 to 1.500 Å. Compared with the corresponding values in a neutral species, we find that the C–O bond shortens by 0.069–0.084 Å and the O–O bond lengthens by 0.146–0.156 Å. The bond angles C–O–O in a neutral species and in an anion range from 111.6° to 111.7° and 107.0° to 107.5°, respectively. That is, the bond angle decreases by about 4.1–4.6°. There are no experimental geometry data for comparison.

Our theoretical EAs for the $n\text{-C}_4\text{H}_9\text{OO}$ radical at various levels are shown in Table 1. The value of EAad is predicted to be 0.831 to 1.574 eV by the seven DFT methods, with ZPVE corrections. The BHLYP method predicts the smallest value; B3P86 results in the biggest. The calculated VDE ranges from 0.966 to 1.267 eV.

Our theoretical harmonic vibrational frequencies of both neutral radical $n\text{-C}_4\text{H}_9\text{OO}$ and anion $n\text{-C}_4\text{H}_9\text{OO}^-$ are listed in Table 9. The values of the BLYP, BPW91, and BP86 methods are very similar, whereas those of the three hybrid DFT methods are consistent with each other. The BHLYP method still calculates the largest value.

E. $n\text{-C}_5\text{H}_{11}\text{OO}$ and $n\text{-C}_5\text{H}_{11}\text{OO}^-$. Burgess, SenSharma, et al. tested the ionization energy of the pentyl peroxy radical to be 7.9 ± 0.2 eV by mass spectrometry in 1968.⁶⁴ From then on, as far as we know, there are no structural or energy-relating studies reported.

The optimized geometries of the ground state of $n\text{-C}_5\text{H}_{11}\text{OO}$ and $n\text{-C}_5\text{H}_{11}\text{OO}^-$ are given in Figure 1 and Table 10. We calculated two possible structures (C_s symmetry and C_1 symmetry) for the neutral radical and anion and find that the C_1 symmetry structure is more stable than the C_s symmetry

TABLE 9: Harmonic Frequencies (ω/cm^{-1}) for the $n\text{-C}_4\text{H}_9\text{OO}$ and the Corresponding Anion $n\text{-C}_4\text{H}_9\text{OO}^-$

		B3LYP	BLYP	BHLYP	B3PW91	BPW91	B3P86	BP86	exptl
		$n\text{-C}_4\text{H}_9\text{OO}$							
a'	ω_1	3123	3040	3221	3137	3062	3139	3044	
a''	ω_2	3108	3027	3201	3132	3062	3136	3043	
	ω_3	3103	3021	3196	3125	3055	3128	3036	
	ω_4	3082	2999	3177	3104	3032	3107	3013	
	ω_5	3067	2984	3164	3087	3014	3089	2994	
	ω_6	3060	2977	3157	3072	2999	3075	2980	
	ω_7	3035	2955	3129	3053	2982	3056	2964	
	ω_8	3029	2952	3122	3045	2977	3048	2960	
	ω_9	3027	2947	3119	3044	2974	3047	2955	
	ω_{10}	1502	1463	1558	1498	1460	1498	1452	
	ω_{11}	1493	1456	1552	1490	1454	1490	1446	
	ω_{12}	1487	1447	1546	1483	1445	1483	1437	
	ω_{13}	1484	1435	1541	1480	1432	1480	1425	
	ω_{14}	1468	1427	1525	1463	1423	1463	1415	
	ω_{15}	1411	1370	1477	1410	1367	1412	1360	
	ω_{16}	1405	1353	1465	1404	1358	1404	1352	
	ω_{17}	1378	1326	1445	1376	1326	1376	1320	
	ω_{18}	1328	1288	1380	1325	1288	1325	1281	
	ω_{19}	1317	1279	1370	1314	1276	1314	1269	
	ω_{20}	1267	1227	1321	1268	1229	1268	1223	
	ω_{21}	1226	1180	1312	1245	1184	1250	1178	
	ω_{22}	1211	1119	1285	1227	1148	1227	1144	
	ω_{23}	1152	1091	1209	1154	1111	1156	1107	
	ω_{24}	1132	1087	1185	1136	1095	1138	1091	
	ω_{25}	1068	1025	1119	1080	1043	1083	1040	
	ω_{26}	1026	982	1078	1040	1000	1044	997	
	ω_{27}	957	926	1002	956	926	956	921	
	ω_{28}	937	879	993	947	893	948	889	
	ω_{29}	837	803	877	844	814	847	811	
	ω_{30}	817	773	858	820	783	821	780	
	ω_{31}	731	703	761	730	706	731	703	
	ω_{32}	556	528	585	560	535	562	534	
	ω_{33}	377	360	396	380	364	381	364	
	ω_{34}	304	291	317	303	291	304	291	
	ω_{35}	250	243	260	250	243	250	242	
	ω_{36}	236	229	245	236	230	236	229	
	ω_{37}	120	113	127	120	114	121	114	
	ω_{38}	78	76	82	79	77	79	76	
	ω_{39}	56	52	63	57	54	57	53	
		$n\text{-C}_4\text{H}_9\text{OO}^-$							
a	ω_1	3095	3009	3192	3114	3040	3117	3021	
	ω_2	3070	2984	3164	3094	3020	3098	3002	
	ω_3	3057	2968	3151	3080	3003	3083	2985	
	ω_4	3029	2950	3124	3050	2980	3053	2959	
	ω_5	3012	2930	3106	3032	2960	3035	2940	
	ω_6	3002	2916	3094	3017	2943	3020	2925	
	ω_7	2984	2903	3076	3003	2932	3005	2912	
	ω_8	2886	2813	3006	2894	2813	2900	2796	
	ω_9	2860	2757	2983	2870	2768	2873	2744	
	ω_{10}	1499	1457	1560	1494	1454	1494	1447	
	ω_{11}	1497	1449	1554	1493	1448	1493	1439	
	ω_{12}	1486	1446	1540	1483	1444	1483	1436	
	ω_{13}	1482	1439	1537	1478	1437	1478	1429	
	ω_{14}	1459	1416	1518	1455	1413	1454	1404	
	ω_{15}	1391	1350	1452	1388	1346	1389	1339	
	ω_{16}	1376	1326	1441	1375	1327	1376	1321	
	ω_{17}	1354	1304	1423	1351	1301	1350	1294	
	ω_{18}	1308	1270	1359	1306	1270	1306	1263	
	ω_{19}	1299	1259	1353	1292	1253	1292	1246	
	ω_{20}	1253	1213	1305	1253	1215	1253	1208	
	ω_{21}	1208	1166	1265	1207	1165	1207	1158	
	ω_{22}	1181	1126	1247	1192	1137	1195	1133	
	ω_{23}	1152	1106	1206	1156	1116	1158	1112	
	ω_{24}	1096	1033	1155	1108	1058	1112	1056	
	ω_{25}	1040	990	1087	1054	1013	1057	1010	
	ω_{26}	969	932	1013	975	939	977	935	
	ω_{27}	961	930	999	959	931	959	925	
	ω_{28}	890	824	955	910	844	915	844	
	ω_{29}	837	806	873	844	816	846	814	

TABLE 9 Continued

	B3LYP	BLYP	BHLYP	B3PW91	BPW91	B3P86	BP86	exptl
ω_{30}	809	766	849	813	778	813	775	
ω_{31}	734	708	762	733	709	733	706	
ω_{32}	540	519	564	543	523	544	522	
ω_{33}	344	331	361	347	335	349	335	
ω_{34}	303	294	317	303	293	304	293	
ω_{35}	258	252	267	257	251	258	251	
ω_{36}	237	227	247	237	228	237	227	
ω_{37}	120	122	128	120	120	120	119	
ω_{38}	93	95	97	95	95	96	95	
ω_{39}	78	76	80	78	78	78	77	

TABLE 10: Optimized Geometry for the $n\text{-C}_5\text{H}_{11}\text{OO}$ and the Corresponding Anion $n\text{-C}_5\text{H}_{11}\text{OO}^-$ ^a

	B3LYP	BLYP	BHLYP	B3PW91	BPW91	B3P86	BP86
$n\text{-C}_5\text{H}_{11}\text{OO}$							
$R(1, 2)$	1.535	1.547	1.524	1.529	1.538	1.526	1.539
$R(2, 8)$	1.536	1.548	1.524	1.530	1.540	1.527	1.540
$R(8, 9)$	1.536	1.549	1.525	1.531	1.541	1.528	1.541
$R(9, 12)$	1.522	1.533	1.512	1.518	1.526	1.515	1.526
$R(12, 17)$	1.467	1.495	1.442	1.459	1.482	1.456	1.482
$R(17, 18)$	1.324	1.352	1.301	1.313	1.336	1.313	1.338
$A(1, 2, 8)$	113.0	113.2	112.9	113.0	113.2	112.9	113.0
$A(2, 8, 9)$	113.0	113.1	112.8	112.9	113.1	112.9	113.0
$A(8, 9, 12)$	114.1	114.3	113.9	114.2	114.4	114.0	114.2
$A(9, 12, 17)$	108.0	107.8	108.0	108.1	108.1	107.9	107.9
$A(12, 17, 18)$	111.7	111.6	111.7	111.7	111.7	111.6	111.6
$D(1, 2, 8, 9)$	-179.7	-179.7	-179.7	-179.7	-179.7	-179.7	-179.7
$D(2, 8, 9, 12)$	179.6	179.5	179.6	179.6	179.5	179.8	179.7
$D(8, 9, 12, 17)$	67.0	68.0	66.0	67.0	67.9	66.6	67.6
$D(9, 12, 17, 18)$	-177.3	-177.3	-177.6	-176.9	-176.8	-176.9	-176.8
$n\text{-C}_5\text{H}_{11}\text{OO}^-$							
$R(1, 2)$	1.536	1.549	1.525	1.531	1.540	1.528	1.541
$R(2, 8)$	1.536	1.548	1.524	1.530	1.540	1.527	1.540
$R(8, 9)$	1.535	1.548	1.524	1.530	1.540	1.527	1.540
$R(9, 12)$	1.539	1.550	1.526	1.533	1.543	1.530	1.544
$R(12, 17)$	1.389	1.412	1.373	1.383	1.400	1.381	1.400
$R(17, 18)$	1.480	1.497	1.454	1.464	1.479	1.462	1.481
$A(1, 2, 8)$	113.4	113.6	113.2	113.4	113.6	113.3	113.5
$A(2, 8, 9)$	113.9	113.9	113.7	113.9	113.9	113.8	113.9
$A(8, 9, 12)$	113.4	113.7	113.3	113.3	113.5	113.1	113.2
$A(9, 12, 17)$	109.5	109.4	109.7	109.6	109.5	109.5	109.3
$A(12, 17, 18)$	107.2	107.6	107.3	107.1	107.3	107.0	107.2
$D(1, 2, 8, 9)$	-180.0	179.9	-179.8	-180.0	179.8	-179.9	179.8
$D(2, 8, 9, 12)$	-179.8	177.7	-179.0	-179.5	178.4	-179.5	178.2
$D(8, 9, 12, 17)$	60.9	60.3	61.0	60.8	60.1	60.3	59.3
$D(9, 12, 17, 18)$	178.9	176.6	179.7	179.2	177.6	179.1	177.1

^a All bond distances are in angstroms, all bond angles are in degrees, and all results were obtained with the DZP++ basis set.

structure in energy by approximately 0.02 eV. Therefore, the C_s symmetry structure is a local minimal point on the potential energy surface.

In the neutral radical $n\text{-C}_5\text{H}_{11}\text{OO}$, the bond distances of the three C–C bonds nonadjacent to the C–O bond are very close to each other; the adjacent one is shorter by about 0.015 Å. This trend also occurs in $n\text{-C}_3\text{H}_7\text{OO}$ and $n\text{-C}_4\text{H}_9\text{OO}$. The bond length values of C–O calculated from the seven methods range from 1.442 to 1.495 Å, whereas those of the O–O bond range from 1.301 to 1.352 Å. For the anion $n\text{-C}_5\text{H}_{11}\text{OO}^-$, three distant C–C bonds are very similar to each other in length, as well as those in the neutral species. The theoretical C–O bond distances are in the range from 1.373 to 1.412 Å (shortening by about 0.069–0.083 Å); C–C bond distances are in the range from 1.454 to 1.497 Å (lengthening by about 0.143–0.156 Å). They are in the same way very close to those in $n\text{-C}_3\text{H}_7\text{OO}^-$ and $n\text{-C}_4\text{H}_9\text{OO}^-$. The C–O–O bond angle is about 111.6–111.7° in the neutral species, whereas it is 107.0–107.6° in the anion

(decreased about 4.0–4.6°). The dihedral angle C–C–O–O is about 176.6–179.7°.

The theoretical EAad and VDE are listed in Table 1. The range of the EAad is from 0.837 to 1.581 eV by the seven DFT functionals. The B3P86 method predicts the largest corrected EAad (1.581 eV), and the BHLYP method predicts the smallest (0.837 eV).

Theoretical harmonic vibrational frequencies by the seven DFT functionals for the neutral radical $n\text{-C}_5\text{H}_{11}\text{OO}$ and anion $n\text{-C}_5\text{H}_{11}\text{OO}^-$ are given in Table 11. The BLYP, BPW91, and BP86 methods give close values. The same is true of the values of the three hybrid DFT methods. The BHLYP method still produces the largest value.

F. $i\text{-C}_3\text{H}_7\text{OO}$ and $i\text{-C}_3\text{H}_7\text{OO}^-$. In the past decades, a variety of studies of the isopropyl peroxy radical have been done on IR and UV absorptions spectrum and mutual reaction mechanisms.^{38,47,55,59–62,65} For example, Adachi and Basco observed the transient absorption spectra and measured the rate constants for the mutual

TABLE 11: Harmonic Frequencies (ω/cm^{-1}) for the $n\text{-C}_5\text{H}_{11}\text{OO}$ and the Corresponding Anion $n\text{-C}_5\text{H}_{11}\text{OO}^-$

		B3LYP	BLYP	BHLYP	B3PW91	BPW91	B3P86	BP86	exptl
		$n\text{-C}_5\text{H}_{11}\text{OO}$							
a'	ω_1	3122	3039	3221	3137	3062	3139	3043	
a''	ω_2	3105	3024	3198	3128	3058	3133	3041	
	ω_3	3099	3019	3193	3122	3053	3126	3034	
	ω_4	3085	3002	3181	3106	3033	3108	3013	
	ω_5	3067	2984	3163	3087	3014	3089	2994	
	ω_6	3059	2977	3157	3072	2999	3075	2980	
	ω_7	3047	2965	3143	3069	2997	3071	2976	
	ω_8	3034	2953	3129	3051	2980	3054	2961	
	ω_9	3029	2952	3119	3044	2977	3048	2960	
	ω_{10}	3019	2939	3113	3038	2968	3040	2949	
	ω_{11}	3014	2934	3109	3032	2962	3034	2943	
	ω_{12}	1504	1465	1559	1499	1461	1499	1454	
	ω_{13}	1493	1455	1551	1489	1453	1489	1445	
	ω_{14}	1491	1452	1546	1487	1449	1487	1441	
	ω_{15}	1484	1440	1545	1480	1439	1480	1431	
	ω_{16}	1481	1435	1537	1478	1432	1477	1425	
	ω_{17}	1467	1426	1525	1463	1423	1462	1415	
	ω_{18}	1412	1370	1480	1412	1367	1414	1360	
	ω_{19}	1408	1354	1469	1407	1360	1407	1354	
	ω_{20}	1384	1334	1451	1383	1336	1384	1329	
	ω_{21}	1364	1318	1423	1360	1316	1360	1309	
	ω_{22}	1324	1286	1374	1323	1287	1322	1280	
	ω_{23}	1311	1272	1363	1311	1274	1310	1267	
	ω_{24}	1290	1252	1342	1285	1248	1285	1241	
	ω_{25}	1247	1207	1314	1250	1209	1253	1203	
	ω_{26}	1219	1174	1300	1242	1177	1244	1171	
	ω_{27}	1211	1121	1275	1218	1148	1219	1144	
	ω_{28}	1155	1094	1212	1157	1113	1158	1109	
	ω_{29}	1133	1088	1186	1138	1099	1140	1095	
	ω_{30}	1079	1037	1125	1091	1056	1094	1053	
	ω_{31}	1055	1013	1105	1068	1031	1071	1028	
	ω_{32}	1023	982	1076	1031	992	1034	988	
	ω_{33}	965	917	1020	972	926	973	922	
	ω_{34}	927	894	965	933	904	934	900	
	ω_{35}	869	829	919	877	835	878	832	
	ω_{36}	860	816	897	862	829	862	826	
	ω_{37}	765	734	799	765	738	766	734	
	ω_{38}	728	703	755	727	704	727	702	
	ω_{39}	550	520	579	554	528	556	527	
	ω_{40}	400	387	417	399	386	399	385	
	ω_{41}	357	341	374	360	346	361	346	
	ω_{42}	283	272	296	283	272	284	272	
	ω_{43}	237	230	246	238	232	238	231	
	ω_{44}	189	182	197	188	182	188	181	
	ω_{45}	133	127	139	133	128	133	128	
	ω_{46}	84	80	90	85	82	85	81	
	ω_{47}	69	67	72	70	67	69	67	
	ω_{48}	51	47	57	52	49	52	49	
		$n\text{-C}_5\text{H}_{11}\text{OO}^-$							
a	ω_1	3089	3001	3184	3111	3035	3114	3016	
	ω_2	3079	2992	3175	3100	3025	3104	3007	
	ω_3	3076	2987	3169	3099	3024	3101	3004	
	ω_4	3032	2950	3128	3052	2980	3054	2960	
	ω_5	3026	2943	3121	3049	2976	3052	2956	
	ω_6	3013	2928	3105	3028	2954	3032	2937	
	ω_7	3002	2922	3096	3022	2951	3023	2930	
	ω_8	2996	2912	3091	3014	2939	3016	2919	
	ω_9	2984	2905	3077	3003	2934	3006	2913	
	ω_{10}	2886	2814	3006	2894	2815	2900	2797	
	ω_{11}	2861	2773	2984	2871	2780	2873	2751	
	ω_{12}	1501	1460	1560	1496	1457	1496	1449	
	ω_{13}	1497	1449	1556	1494	1447	1494	1438	
	ω_{14}	1489	1447	1545	1484	1445	1484	1437	
	ω_{15}	1487	1446	1540	1483	1444	1483	1436	
	ω_{16}	1476	1432	1532	1473	1431	1472	1422	
	ω_{17}	1459	1417	1518	1455	1413	1454	1404	
	ω_{18}	1397	1354	1457	1393	1351	1393	1344	
	ω_{19}	1385	1332	1453	1386	1337	1388	1330	
	ω_{20}	1356	1309	1425	1354	1308	1354	1300	

TABLE 11 Continued

	B3LYP	BLYP	BHLYP	B3PW91	BPW91	B3P86	BP86	exptl
$\omega 21$	1348	1303	1407	1342	1297	1342	1289	
$\omega 22$	1307	1270	1358	1305	1269	1304	1261	
$\omega 23$	1300	1263	1351	1299	1263	1299	1256	
$\omega 24$	1270	1234	1321	1263	1226	1262	1219	
$\omega 25$	1237	1198	1291	1238	1199	1238	1192	
$\omega 26$	1206	1164	1262	1204	1163	1205	1157	
$\omega 27$	1182	1129	1246	1191	1137	1194	1132	
$\omega 28$	1151	1104	1205	1155	1114	1158	1111	
$\omega 29$	1094	1035	1156	1106	1055	1110	1052	
$\omega 30$	1072	1020	1116	1083	1042	1087	1038	
$\omega 31$	1037	997	1081	1048	1013	1051	1009	
$\omega 32$	989	955	1031	990	958	990	951	
$\omega 33$	922	888	972	928	898	930	895	
$\omega 34$	911	860	959	925	869	929	863	
$\omega 35$	867	836	907	872	841	874	836	
$\omega 36$	852	794	897	861	812	862	803	
$\omega 37$	765	737	798	765	740	766	736	
$\omega 38$	729	705	755	727	705	728	702	
$\omega 39$	532	512	556	535	517	537	516	
$\omega 40$	399	388	415	398	387	399	386	
$\omega 41$	328	316	343	331	319	333	320	
$\omega 42$	282	271	296	282	270	282	270	
$\omega 43$	238	234	246	238	234	238	234	
$\omega 44$	200	195	207	199	194	199	194	
$\omega 45$	133	127	141	133	128	134	128	
$\omega 46$	93	94	98	95	95	95	95	
$\omega 47$	75	74	78	75	73	75	73	
$\omega 48$	68	68	70	68	69	69	69	

TABLE 12: Optimized Geometry for $i\text{-C}_3\text{H}_7\text{OO}$ and the Corresponding Anion $i\text{-C}_3\text{H}_7\text{OO}^-$ ^a

	B3LYP	BLYP	BHLYP	B3PW91	BPW91	B3P86	BP86
$i\text{-C}_3\text{H}_7\text{OO}$							
$R(1, 2)$	1.525	1.536	1.515	1.520	1.528	1.517	1.528
$R(2, 6)$	1.523	1.534	1.513	1.518	1.527	1.516	1.527
$R(2, 11)$	1.480	1.512	1.452	1.472	1.499	1.469	1.500
$R(11, 12)$	1.324	1.351	1.300	1.313	1.335	1.312	1.337
$A(1, 2, 6)$	114.4	114.9	113.9	114.4	114.8	114.3	114.8
$A(1, 2, 11)$	109.2	108.9	109.6	109.3	109.1	109.3	109.0
$A(6, 2, 11)$	105.3	105.0	105.5	105.4	105.1	105.3	105.0
$A(2, 11, 12)$	112.0	111.9	112.0	112.0	112.0	111.9	111.9
$D(1, 2, 11, 12)$	71.8	71.8	71.5	71.2	70.7	70.2	69.7
$D(6, 2, 11, 12)$	-164.8	-164.7	-165.4	-165.4	-165.6	-166.5	-166.8
$i\text{-C}_3\text{H}_7\text{OO}^-$							
$R(1, 2)$	1.541	1.553	1.529	1.535	1.545	1.532	1.544
$R(2, 6)$	1.537	1.550	1.526	1.532	1.541	1.529	1.542
$R(2, 11)$	1.399	1.418	1.381	1.394	1.410	1.392	1.411
$R(11, 12)$	1.483	1.511	1.456	1.466	1.488	1.464	1.489
$A(1, 2, 6)$	112.0	112.2	111.6	112.1	112.4	112.1	112.5
$A(1, 2, 11)$	112.0	112.2	111.9	111.9	112.0	111.7	111.8
$A(2, 11, 12)$	108.1	108.4	108.2	108.0	108.2	107.9	108.1
$A(6, 2, 11)$	107.4	107.0	107.7	107.5	107.1	107.5	107.1
$D(1, 2, 11, 12)$	66.0	64.9	66.9	65.2	64.0	64.7	63.4
$D(6, 2, 11, 12)$	-170.7	-171.6	-170.0	-171.3	-172.3	-171.9	-173.0

^a All bond distances are in angstroms, all bond angles are in degrees, and all results were obtained with the DZP++ basis set.

reaction in 1982.⁶⁰ Chettur and Snelson reported the matrix IR spectra results and vibrational frequencies assignment.⁵⁹

Our calculations predict a C_1 symmetry structure for the ground state of the neutral radical $i\text{-C}_3\text{H}_7\text{OO}$ shown in Table 12 and Figure 1. The bond distance of C–O is in the range from 1.452 to 1.512 Å, a little longer (0.012–0.020 Å) than that in $n\text{-C}_3\text{H}_7\text{OO}$. The O–O bond length is from 1.300 to 1.351 Å (~0.001 Å shorter than that in $n\text{-C}_3\text{H}_7\text{OO}$). It is noteworthy that the geometries obtained via all seven functionals are all similar, showing only slight variations in bond lengths and angles. Among the various functionals, the three hybrid methods (B3LYP, B3P86, and B3PW91) give bond length values that

are generally in agreement with each other. In addition, the bond length values of the BP86 and BPW91 methods are also consistent. In particular, the BHLYP method gives the shortest bond lengths, whereas BLYP predicts the longest bond lengths. The C–O–O bond angle values are 111.9–112.0°, only a little deviation from each other.

The anion $i\text{-C}_3\text{H}_7\text{OO}^-$ has C_1 symmetry, with the C–O and O–O bond distances predicted to be 1.381–1.418 and 1.456–1.511, respectively, by the different DFT methods. In general, the C–O bond length is shorter and the O–O bond length is longer as compared with corresponding neutral radical. We also find two C–C bonds near the C–O bond are very close

TABLE 13: Harmonic frequencies(ω/cm^{-1}) for the *i*-C₃H₇OO and the Corresponding Anion *i*-C₃H₇OO⁻

		B3LYP	BLYP	BHLYP	B3PW91	BPW91	B3P86	BP86	exptl ^a
		<i>i</i> -C ₃ H ₇ OO							
<i>a'</i>	ω_1	3140	3059	3232	3161	3090	3164	3072	
<i>a''</i>	ω_2	3132	3051	3225	3155	3084	3159	3066	
	ω_3	3129	3046	3223	3151	3081	3155	3062	
	ω_4	3119	3037	3212	3143	3073	3147	3054	
	ω_5	3081	3000	3179	3094	3020	3095	3000	
	ω_6	3050	2973	3140	3064	2997	3067	2979	
	ω_7	3045	2968	3135	3060	2992	3063	2975	
	ω_8	1503	1464	1558	1500	1462	1500	1454	
	ω_9	1485	1445	1540	1482	1444	1481	1436	
	ω_{10}	1480	1442	1534	1476	1439	1476	1431	
	ω_{11}	1474	1435	1529	1471	1433	1470	1425	
	ω_{12}	1415	1372	1474	1410	1368	1411	1361	
	ω_{13}	1400	1353	1465	1397	1350	1397	1343	
	ω_{14}	1352	1307	1412	1349	1308	1350	1301	1372
	ω_{15}	1334	1278	1404	1334	1281	1334	1274	1310
	ω_{16}	1215	1152	1314	1248	1158	1253	1154	1101
	ω_{17}	1190	1125	1241	1191	1152	1192	1147	1178
	ω_{18}	1155	1098	1213	1165	1122	1168	1118	1153
	ω_{19}	1118	1058	1183	1122	1069	1124	1065	1130
	ω_{20}	945	914	985	945	916	946	911	
	ω_{21}	933	906	968	930	904	929	899	
	ω_{22}	894	845	956	906	862	910	859	884
	ω_{23}	794	721	854	807	743	810	742	789
	ω_{24}	518	485	548	524	495	525	494	515
	ω_{25}	445	426	468	446	428	447	427	450
	ω_{26}	340	328	355	339	328	339	326	348
	ω_{27}	300	284	316	300	285	300	284	305
	ω_{28}	235	225	248	237	229	238	228	
	ω_{29}	194	184	205	196	188	195	185	
	ω_{30}	99	91	108	100	93	103	96	
		<i>i</i> -C ₃ H ₇ OO ⁻							
<i>a</i>	ω_1	3114	3022	3221	3124	3036	3124	3017	
	ω_2	3085	3002	3180	3108	3035	3111	3013	
	ω_3	3072	2993	3163	3096	3028	3100	3009	
	ω_4	3045	2962	3137	3071	2999	3074	2979	
	ω_5	3006	2930	3096	3021	2953	3024	2935	
	ω_6	2984	2902	3077	2999	2924	3001	2906	
	ω_7	2881	2775	3004	2889	2786	2891	2765	
	ω_8	1497	1455	1553	1493	1452	1492	1444	
	ω_9	1478	1438	1534	1474	1434	1473	1426	
	ω_{10}	1463	1423	1519	1458	1419	1458	1410	
	ω_{11}	1452	1411	1509	1447	1407	1447	1398	
	ω_{12}	1370	1325	1434	1367	1321	1368	1314	
	ω_{13}	1359	1311	1424	1357	1312	1357	1305	
	ω_{14}	1330	1288	1392	1319	1274	1317	1266	
	ω_{15}	1304	1255	1370	1300	1253	1301	1247	
	ω_{16}	1196	1137	1268	1208	1152	1212	1148	
	ω_{17}	1160	1116	1214	1159	1119	1161	1115	
	ω_{18}	1120	1073	1174	1126	1084	1130	1081	
	ω_{19}	959	904	1031	969	913	972	910	
	ω_{20}	925	881	968	929	890	932	887	
	ω_{21}	893	864	930	890	862	891	858	
	ω_{22}	854	800	912	872	824	876	824	
	ω_{23}	801	751	845	811	773	814	771	
	ω_{24}	490	469	512	494	476	496	475	
	ω_{25}	462	446	481	463	448	464	448	
	ω_{26}	337	326	352	334	322	334	321	
	ω_{27}	288	273	304	290	276	291	276	
	ω_{28}	223	213	236	224	216	224	216	
	ω_{29}	201	191	210	202	192	202	191	
	ω_{30}	151	142	156	156	148	159	150	

^a See ref 67.

to the corresponding C–C bonds in C₂H₅OO, *n*-C₃H₇OO, *n*-C₄H₉OO, and *n*-C₅H₁₁OO, but getting longer by about 0.014–0.017 Å as compared with those in the neutral species. The C–O–O bond angle values are getting less by about 3.5–4.0° than that in the neutral species.

Our theoretical EAad and VDE are listed in Table 1. The EAad values range from 0.805 to 1.552 eV, with ZPVE corrections. The B3P86 method predicts the largest value; the BHLYP method gives the smallest. No experimental data are available for comparison, but Stark presented a G2MP2

TABLE 14: Optimized Geometry for the $t\text{-C}_4\text{H}_9\text{OO}$ and the Corresponding Anion $t\text{-C}_4\text{H}_9\text{OO}^-$ ^a

	B3LYP	BLYP	BHLYP	B3PW91	BPW91	B3P86	BP86
$t\text{-C}_4\text{H}_9\text{OO}$							
$R(1, 2)$	1.529	1.539	1.519	1.524	1.532	1.521	1.532
$R(2, 6)$	1.529	1.539	1.519	1.524	1.532	1.521	1.532
$R(2, 7)$	1.528	1.538	1.518	1.523	1.531	1.520	1.531
$R(2, 14)$	1.502	1.543	1.468	1.493	1.528	1.490	1.528
$R(14, 15)$	1.321	1.347	1.299	1.310	1.331	1.310	1.333
$A(1, 2, 6)$	112.5	112.8	112.3	112.4	112.7	112.4	112.7
$A(1, 2, 7)$	112.5	113.1	112.1	112.5	113.0	112.5	113.0
$A(1, 2, 14)$	108.0	107.5	108.5	108.1	107.6	108.0	107.5
$A(7, 2, 14)$	102.5	102.0	102.9	102.7	102.2	102.7	102.2
$A(2, 14, 15)$	113.3	113.3	113.2	113.2	113.3	113.1	113.1
$D(1, 2, 14, 15)$	-61.0	-60.9	-61.1	-61.0	-60.8	-60.9	-60.8
$D(7, 2, 14, 15)$	180.0	180.0	180.0	180.0	180.0	180.0	180.0
$t\text{-C}_4\text{H}_9\text{OO}^-$							
$R(1, 2)$	1.545	1.558	1.533	1.539	1.549	1.536	1.549
$R(2, 6)$	1.545	1.558	1.533	1.539	1.549	1.536	1.549
$R(2, 7)$	1.539	1.551	1.528	1.533	1.542	1.530	1.542
$R(2, 14)$	1.417	1.440	1.395	1.411	1.432	1.410	1.434
$R(14, 15)$	1.486	1.519	1.457	1.468	1.493	1.466	1.494
$A(1, 2, 6)$	110.1	110.3	109.9	110.0	110.3	110.1	110.3
$A(1, 2, 7)$	110.5	110.8	110.1	110.7	111.1	110.8	111.2
$A(1, 2, 14)$	110.2	110.0	110.5	110.1	109.7	109.9	109.5
$A(7, 2, 14)$	105.2	104.8	105.5	105.3	105.0	105.3	104.9
$A(2, 14, 15)$	110.0	109.9	110.1	109.8	109.7	109.6	109.5
$D(1, 2, 14, 15)$	-60.9	-60.8	-61.0	-60.7	-60.6	-60.7	-60.6
$D(7, 2, 14, 15)$	-180.0	180.0	-180.0	180.0	180.0	180.0	180.0

^a All bond distances are in angstroms, all bond angles are in degrees, and all results were obtained with the DZP++ basis set.

theoretical value to be 1.196 eV,⁶⁶ very close to our BP86 result. The VDE are in the range from 1.257 to 1.970 eV.

Chettur and Snelson detected the infrared spectra of the $t\text{-C}_3\text{H}_7\text{OO}$ radical, and a partial vibrational frequency assignment was made.⁶⁷ Our theoretical harmonic vibrational frequencies and some corresponding experimental values are presented in Table 13. The BHLYP method always gives the largest values. The B3LYP, B3PW91, and B3P86 methods predict close values, always a little larger than those from BLYP, BPW91, and BP86 methods. Compared with experimental values, all of our theoretical O–O stretch frequency values are larger by an average absolute percent deviation of 4.6–19.3%. The BLYP method gives the best agreement with the experimental result. For the other frequencies, we can rank the methods according to average absolute percent deviation from experiment: B3LYP (0.8%), B3PW91 (1.1%), B3P86 (1.2%), BPW91 (2.9%), BP86 (3.2%), BHLYP (3.6%), and BLYP (3.7%). Theoretical harmonic vibrational frequencies for the neutral radical show good agreement with the experimental results.

F. $t\text{-C}_4\text{H}_9\text{OO}$ and $t\text{-C}_4\text{H}_9\text{OO}^-$. The *tert*-butyl peroxy radical ($t\text{-C}_4\text{H}_9\text{OO}$) as a significant intermediate in many reactions has been carefully studied for its thermochemistry and kinetic properties.^{40,47,48,68–70} Recently, Clifford, Wenthold, et al. reported the photoelectron spectroscopy, gas phase acidity, and thermochemistry of *tert*-butyl hydroperoxide. The results suggested that the ground state of $t\text{-C}_4\text{H}_9\text{OO}$ is a $^2A''$ state. The electron affinity of $t\text{-C}_4\text{H}_9\text{OO}$ was determined via negative ion photoelectron spectroscopy to be $1.196 \pm 0.011\text{eV}$.⁶⁸

Our optimized geometries for the *tert*-butyl peroxy radical and its anion are shown in Figure 1. The parameters are displayed in Table 14. Harmonic vibrational frequencies for both species are given in Table 15. The theoretical predictions support a C_s symmetry structure with a $^2A''$ ground state for the *tert*-butyl peroxy radical. The bond distances of C–O and O–O for $t\text{-C}_4\text{H}_9\text{OO}$ are in the range from 1.468 to 1.543 and 1.299 to 1.347 Å, respectively. Three C–C bonds are very similar to

each other. The C–O–O bond angle values from the seven DFT methods are about 113.1–113.3°. When an extra electron attaches to the radical, we find that the symmetry remains C_s , but the ground state become $^1A'$. Remarkable changes in the bond distances of C–O and O–O for $t\text{-C}_4\text{H}_9\text{OO}^-$ also take place. The C–O bond becomes shorter by about 0.073–0.103 Å while the O–O bond gets longer by about 0.156–0.172 Å. The C–O–O bond angle values decrease by ~ 3.1 – 3.6° as compared to that in the neutral species.

The theoretical EAad and VDE, as well as the experimental electron affinity data, are listed in Table 1. The range of EAad is from 0.791 to 1.537 eV obtained via the seven different functionals. Compared with the experimental data determined by Clifford, Wenthold, et al.,⁶⁸ the BP86 method (1.114 eV) predicts the most reliable and reasonable value; the absolute error is only 0.082 eV. The B3P86 method predicts the largest corrected EAad (1.537 eV), which deviates 0.341 eV higher, whereas the BHLYP method predicts the smallest corrected EAad (0.791 eV), which deviates 0.405 eV lower.

A number of articles about the vibrational frequencies of *tert*-butyl peroxy radical have been reported in the literature.^{68–70} Early in 1975, Parkes and Donovan detected an infrared absorption spectrum in gas phase and assigned two vibrational mode frequencies: $760 \pm 2\text{ cm}^{-1}$ (C–C stretching) and $693.7 \pm 0.5\text{ cm}^{-1}$ (C–O stretching).⁶⁹ Later, in 1987, Chettur and Snelson studied the infrared spectrum in matrix Ar and gave nine vibrational mode frequencies involving C–C stretching ($808 \pm 2\text{ cm}^{-1}$) and C–O stretching ($730 \pm 2\text{ cm}^{-1}$).⁷⁰ In 1998, Clifford et al. obtained two vibrational frequencies of the ground state, that is, $1130 \pm 90\text{ cm}^{-1}$ (O–O stretching) and $245 \pm 90\text{ cm}^{-1}$ (Skel. bending).⁶⁸ Comparing with available experimental data of Clifford et al., Chettur and Snelson, and Parkes and Donovan, we find excellent agreement and can rank the functionals according to average absolute percent error from experiment: BPW91 (2.2%), BP86 (2.3%), B3LYP (2.4%), BPW91 (2.2%), BLYP (2.8%), B3PW91 (2.9%), B3P86 (3.1%),

TABLE 15: Harmonic Frequencies(ω/cm^{-1}) for the $t\text{-C}_4\text{H}_9\text{OO}$ and the Corresponding Anion $t\text{-C}_4\text{H}_9\text{OO}^-$

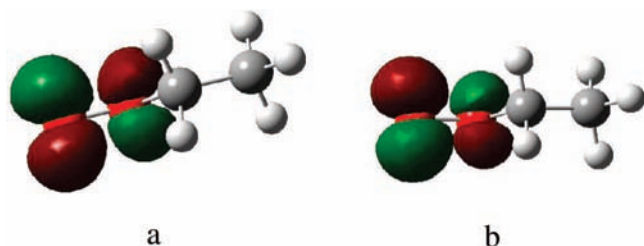
		B3LYP	BLYP	BHLYP	B3PW91	BPW91	B3P86	BP86	exptl ^a
		$t\text{-C}_4\text{H}_9\text{OO}$							
a'	ω_1	3143	3061	3236	3162	3090	3165	3071	
	ω_2	3130	3046	3224	3152	3081	3155	3061	
	ω_3	3122	3039	3215	3146	3075	3149	3056	
	ω_4	3054	2977	3144	3066	2998	3069	2980	
	ω_5	3047	2969	3136	3060	2993	3063	2975	
	ω_6	1514	1474	1569	1511	1472	1510	1464	
	ω_7	1490	1450	1547	1488	1449	1488	1441	
	ω_8	1481	1442	1535	1475	1438	1475	1430	
	ω_9	1421	1379	1479	1414	1373	1414	1366	
	ω_{10}	1397	1353	1459	1392	1348	1393	1341	
	ω_{11}	1293	1243	1354	1298	1253	1301	1250	
	ω_{12}	1223	1152	1312	1252	1173	1257	1169	1187 \pm 2
	ω_{13}	1175	1086	1257	1183	1115	1186	1111	1124 \pm 2
	ω_{14}	1045	1009	1090	1044	1012	1045	1007	1130 \pm 90, 1139 \pm 2
	ω_{15}	931	899	971	932	903	933	899	
	ω_{16}	810	751	893	825	769	830	768	808 \pm 2, 760 \pm 2
	ω_{17}	729	658	780	743	682	748	683	730 \pm 2, 693.7 \pm 0.5
	ω_{18}	540	499	574	546	509	548	508	539 \pm 2
	ω_{19}	401	387	417	399	386	399	385	403 \pm 2
	ω_{20}	356	342	372	356	342	356	342	361 \pm 2
	ω_{21}	267	253	280	267	255	268	255	245 \pm 90, 337 \pm 2
	ω_{22}	239	228	254	243	233	243	231	
a''	ω_{23}	3140	3057	3232	3159	3087	3162	3068	
	ω_{24}	3130	3048	3222	3150	3080	3153	3061	
	ω_{25}	3120	3038	3213	3144	3073	3147	3054	
	ω_{26}	3047	2970	3137	3061	2993	3063	2975	
	ω_{27}	1488	1448	1544	1485	1446	1484	1438	
	ω_{28}	1482	1444	1535	1476	1439	1476	1431	
	ω_{29}	1462	1423	1516	1456	1419	1455	1410	
	ω_{30}	1394	1349	1456	1388	1344	1388	1336	
	ω_{31}	1261	1213	1321	1266	1222	1269	1219	
	ω_{32}	1034	998	1080	1032	998	1032	993	
	ω_{33}	961	934	998	956	929	955	924	
	ω_{34}	929	898	968	931	903	932	899	
	ω_{35}	433	412	457	432	413	433	412	
	ω_{36}	328	313	344	328	314	328	313	
	ω_{37}	229	214	248	232	218	231	215	
	ω_{38}	172	165	184	174	166	173	163	
	ω_{39}	121	115	127	123	118	125	119	
		$t\text{-C}_4\text{H}_9\text{OO}^-$							
a	ω_1	3115	3016	3225	3124	3032	3124	3011	
	ω_2	3076	2993	3169	3099	3027	3102	3007	
	ω_3	3063	2980	3155	3087	3016	3090	2996	
	ω_4	3010	2931	3102	3023	2952	3025	2934	
	ω_5	2999	2917	3090	3012	2936	3014	2917	
	ω_6	1506	1463	1563	1501	1459	1501	1451	
	ω_7	1478	1438	1533	1473	1434	1473	1425	
	ω_8	1464	1424	1519	1460	1422	1460	1414	
	ω_9	1374	1331	1435	1368	1325	1368	1318	
	ω_{10}	1342	1297	1409	1332	1284	1331	1276	
	ω_{11}	1254	1204	1313	1260	1217	1264	1214	
	ω_{12}	1218	1155	1300	1223	1161	1226	1156	
	ω_{13}	1031	997	1076	1030	998	1031	993	
	ω_{14}	924	869	1016	940	878	945	876	
	ω_{15}	898	829	941	905	849	908	847	
	ω_{16}	845	781	906	864	813	868	812	
	ω_{17}	738	703	775	748	719	752	719	
	ω_{18}	512	490	535	518	500	521	500	
	ω_{19}	403	390	417	400	388	400	387	
	ω_{20}	351	337	366	350	337	351	337	
	ω_{21}	268	258	279	218	261	272	262	
	ω_{22}	215	212	223	217	216	218	217	
	ω_{23}	3110	3011	3221	3120	3033	3120	3013	
	ω_{24}	3087	3002	3183	3081	3026	3111	3003	
	ω_{25}	3057	2973	3150	3004	3008	3084	2989	
	ω_{26}	2991	2907	3084	3108	2927	3007	2908	
	ω_{27}	1482	1441	1538	1476	1435	1476	1427	
	ω_{28}	1464	1424	1520	1458	1419	1457	1410	
	ω_{29}	1440	1402	1495	1433	1395	1432	1387	

TABLE 15 Continued

	B3LYP	BLYP	BHLYP	B3PW91	BPW91	B3P86	BP86	exptl ^a
ω_{30}	1333	1284	1403	1323	1272	1323	1264	
ω_{31}	1223	1174	1283	1226	1182	1229	1178	
ω_{32}	1012	980	1055	1008	978	1009	974	
ω_{33}	927	902	963	920	896	921	892	
ω_{34}	888	852	931	892	860	895	858	
ω_{35}	459	441	480	458	441	459	441	
ω_{36}	336	323	350	334	322	335	322	
ω_{37}	217	205	234	270	209	217	208	
ω_{38}	173	165	187	174	175	176	177	
ω_{39}	157	157	143	162	155	163	154	

^a See ref 16.TABLE 16: Wiberg Bond Indexes (WBIs) of the C₂H₅OO/ C₂H₅OO⁻ of NBO Analysis

compd	C ₂ H ₅ OO	C ₂ H ₅ OO ⁻
O–O	1.2076	0.9454
C–O	0.8502	0.9728

Figure 2. HUMO of neutral C₂H₅OO (C_s, ²A'') and LUMO of anionic C₂H₅OO⁻ (C_s, ¹A').

and BHLYP (5.2%). The BHLYP method gives the largest frequencies and deviation from experimental results.

Conclusions

In this work, we systematically study the structures, electron affinities, and harmonic vibrational frequencies of seven alkyl peroxy radicals R-OO/R-OO⁻ (R = CH₃, C₂H₅, *n*-C₃H₇, *n*-C₄H₉, *n*-C₅H₁₁, *i*-C₃H₇, and *t*-C₄H₉) with seven carefully selected DFT methods. All the results show some consistent trends listed below: (a) All the bond lengths of O–O in the radicals are a little shorter than those in the corresponding anions (ranging from 0.143 to 0.172 Å), whereas the C–O bond lengths in radicals are a little longer than those in the corresponding anions (ranging from 0.058 to 0.103 Å). This is because when an electron attaches to the radicals, it will enter the antibonding orbital, and as a result, it decreases the bonding interaction of the O–O bond. Taking, for example, C₂H₅OO/C₂H₅OO⁻, the LUMO (shown in Figure 2a) of C₂H₅OO is an antibonding orbital. When the electron attaches to the radical, it will enter this antibonding orbital and form the antibonding HUMO (shown in Figure 2b) of C₂H₅OO⁻. The natural bond orbital (NBO) analysis gives Wiberg bond indexes (WBIs) of the O–O and C–O bonds of C₂H₅OO and C₂H₅OO⁻ shown in Table 16. From the results, we can see that the change of the WBIs also agrees with the change in the bond lengths. The C–C bond length near the C–O bond increases while the other C–C bonds are almost unchanged when an extra electron is attached to the radical. (b) The bond angle C–O–O in the radical is less than that in the anion by ~3.1–5.0°, and the C–C–C bond angles near atom O are the same, whereas the C–C–O bond angle and other C–C–C bond angles are a little bigger.

In the prediction of bond lengths, the seven methods consistently follow the order BLYP > BP86 BPW91 > B3LYP > B3PW91 ~ B3P86 > BHLYP. The BLYP method always provides the longest bond lengths, and the BHLYP predicts the shortest. All seven methods predict very close bond angle values.

Compared with the limited experimental EAad values, the average absolute errors for all seven DFT methods are 0.04 (BP86), 0.08 (B3LYP), 0.12 (BLYP), 0.18 (BPW91), 0.20 (B3PW91), 0.30 (B3P86), and 0.33 (BHLYP) eV. The BP86 and BLYP methods are the most reliable. The adiabatic EAs (with ZPVE) are predicted by the BP86 method to be 1.150 (CH₃OO), 1.124 (C₂H₅OO), 1.146 (*n*-C₃H₇OO), 1.173 (*n*-C₄H₉OO), 1.184 (*n*-C₅H₁₁OO), 1.145 (*i*-C₃H₇OO), and 1.114 eV (*t*-C₄H₉OO). The B3P86 method always gives the largest values, and the BHLYP method predicts the smallest. Except for the B3P86 method, the other six methods predict EA values that are always smaller than the experimental values.

Comparison of harmonic vibrational frequencies predicted from the seven DFT methods with reliable experimental data can be used to evaluate the performance of the various methods in predicting the vibrational modes of alkyl peroxy radicals. We can rank the methods by total percent difference: BPW91 (1.7%), BP86 (2.1%), B3LYP (2.2%), B3PW91 (2.7%), BLYP (2.8%), B3P86 (3.1%), and BHLYP (7.7%). All the harmonic vibration frequencies show reasonable agreement with available experimental data, excluding BHLYP. The HF/DFT hybrid functionals produce higher vibrational frequencies than the pure DFT exchange functionals, which has also been observed in the present studies.

Acknowledgment.

We thank Prof. Henry F. Schaefer at the Center for Computational Quantum Chemistry, University of Georgia, for his help.

Supporting Information Available: Additional information as noted in text. This material is available free of charge via the Internet at <http://pubs.acs.org>.

References and Notes

- (1) Lightfoot, P. D.; Cox, R. A.; Crowley, J. N.; Destriau, M.; Hayman, G. D.; Jenkin, E.; Moortgat, G. K.; Zabel, F. *Atmos. Environ.* **1992**, *26A*, 1805.
- (2) Wallington, T. J.; Dagaut, P.; Kurylo, M. J. *Chem. Rev.* **1992**, *92*, 667.
- (3) Finlayson-Pitts, B. J.; Pitts, J. N., Jr. *Science* **1997**, *276*, 1045.
- (4) King, M. D.; Thompson, K. C. *Atmos. Environ.* **2003**, *37*, 4517.
- (5) Benson, S. W. *J. Am. Chem. Soc.* **1965**, *87*, 972.
- (6) Fu, H. B.; Hu, Y. J.; Bernstein, E. R. *J. Chem. Phys.* **2006**, *125*, 014310.
- (7) Gardiner, W. C., Ed. *Combustion Chemistry*; Springer-Verlag: New York, 1984.
- (8) Benson, S. W.; Nangia, P. S. *Acc. Chem. Res.* **1979**, *12*, 223.

- (9) Knox, J. H. *Combust. Flame* **1965**, *9*, 297.
- (10) Slagle, I. R.; Ratajczak, E.; Gutman, D. *J. Phys. Chem.* **1986**, *90*, 402.
- (11) Tallman, K. A.; Tronche, C.; Yoo, D. J.; Greenberg, M. M. *J. Am. Chem. Soc.* **1998**, *120*, 4903.
- (12) Porter, N. A.; Mills, K. A.; Carter, R. L. *J. Am. Chem. Soc.* **1994**, *116*, 6690.
- (13) Blanksby, S. J.; Ramond, T. M.; Davico, G. E.; Nimlos, M. R.; Kato, S.; Bierbaum, V. M.; Lineberger, W. C.; Ellison, G. B.; Okumura, M. *J. Am. Chem. Soc.* **2001**, *123*, 9585.
- (14) Nandi, S.; Blanksby, S. J.; Zhang, X.; Nimlos, M. R.; Dayton, D. C.; Ellison, G. B. *J. Phys. Chem. A* **2002**, *106*, 7547.
- (15) Howard, J. A. *Adv. Free Radical Chem.* **1972**, *4*, 49.
- (16) Clifford, E. P.; Wenthold, P. G.; Gareyev, R.; Lineberger, W. C.; Depuy, C. H.; Bierbaum, V. M.; Ellison, G. B. *J. Chem. Phys.* **1998**, *109*, 10293.
- (17) Hohenberg, P.; Kohn, W. *Phys. Rev. B* **1964**, *136*, 864.
- (18) Kohn, W.; Sham, L. J. *Phys. Rev. A* **1965**, *140*, 1133.
- (19) Kohn, W.; Becke, A. D.; Parr, R. G. *J. Phys. Chem.* **1996**, *100*, 12974.
- (20) Xu, W. G.; Gao, A. F. *J. Phys. Chem. A* **2006**, *110*, 997.
- (21) Xu, W. G.; Gao, A. F. *J. Chem. Phys.* **2005**, *123*, 084302.
- (22) Rienstra-Kiracofe, J. C.; Tschumper, G. S.; Schaefer, H. F.; Nandi, S.; Ellison, G. B. *Chem. Rev.* **2002**, *102*, 231.
- (23) Weimer, M.; Sala, F. D.; Gorling, A. *Chem. Phys. Lett.* **2003**, *372*, 538.
- (24) Jensen, F. *J. Chem. Phys.* **2002**, *117*, 9234.
- (25) Mallard, W. G.; Linstrom, P. J., Eds.; *NIST Chemistry WebBook: NIST Standard Reference Database Number 69*; National Institute of Standards and Technology: Gaithersburg, MD, 2000 (Feb); <http://webbook.nist.gov>.
- (26) Becke, A. D. *Phys. Rev. A* **1988**, *38*, 3098.
- (27) Lee, C.; Yang, W.; Parr, R. G. *Phys. Rev. B* **1993**, *37*, 785.
- (28) Becke, A. D. *J. Chem. Phys.* **1993**, *98*, 1372. The BH and HLYP method implemented in the Gaussian programs has the formula $0.5*Ex(LSDA)+0.5*Ex(HF)+0.5*Delta-Ex(B88)+Ec-(LYP)$, which is not precisely the formulation proposed by Becke in his paper.
- (29) Becke, A. D. *J. Chem. Phys.* **1993**, *98*, 5648.
- (30) Perdew, J. P. *Phys. Rev. B* **1986**, *33*, 8822.
- (31) Perdew, J. P.; Wang, Y. *Phys. Rev. B* **1992**, *45*, 13244.
- (32) Frisch, M. J.; Trucks, G. W.; Schlegel, H. B. et al., *GAUSSIAN 98, Revision A.9*; Gaussian, Inc., Pittsburgh PA, 1998.
- (33) Huzinaga, S. *J. Chem. Phys.* **1965**, *42*, 1293.
- (34) Dunning, T. H. *J. Chem. Phys.* **1970**, *53*, 2823.
- (35) Huzinaga, S. *Approximate Atomic Wavefunctions II*, Department of Chemistry, University of Alberta: Edmonton, Alberta, Canada, 1971; Vol. II.
- (36) Dunning, T. H.; Hay, P. J. In *Modern Theoretical Chemistry*; Schaefer, H. F., Ed.; Plenum: New York, 1977; Chapter 1, pp 1–27.
- (37) Lee, T. J.; Schaefer, H. F. *J. Chem. Phys.* **1985**, *83*, 1784.
- (38) Parkes, D. A.; Paul, D. M.; Quinn, C. P.; Robson, R. C. *Chem. Phys. Lett.* **1973**, *23*, 425.
- (39) Hochanadel, C. J.; Ghormley, J. A.; Boyle, J. W.; Ogren, P. J. *J. Phys. Chem.* **1977**, *81*, 3.
- (40) Anastasi, C.; Smith, I. W. M.; Parkes, D. A. *J. Chem. Soc.* **1978**, *74*, 1693 *Faraday Trans. 1*.
- (41) McAdam, K.; Veyret, B.; Lesclaux, R. *Chem. Phys. Lett.* **1987**, *133*, 39.
- (42) Dagaut, P.; Kurylo, M. J. *J. Photochem. Photobiol., A* **1990**, *51*, 133.
- (43) Maricq, M. M.; Wallington, T. J. *J. Phys. Chem.* **1992**, *96*, 986.
- (44) Hunziker, H. E.; Wendt, H. R. *J. Chem. Phys.* **1976**, *64*, 3488.
- (45) Pushkarsky, M. B.; Zalyubovsky, S. J.; Miller, T. A. *J. Chem. Phys.* **2000**, *112*, 10695.
- (46) Ase, P.; Bock, W.; Snelson, A. *J. Phys. Chem.* **1986**, *90*, 2099.
- (47) Jacox, M. E., *Vibrational and electronic energy levels of polyatomic transient molecules*; American Chemical Society: Washington, DC, 1994, 464.
- (48) Jacox, M. E. *Vibrational and electronic energy levels of polyatomic transient molecules: supplement B. J. Phys. Chem. Ref. Data* **2003**, *32* (1), 1–441.
- (49) Hartmann, D.; Karthaus, J.; Zellner, R. *J. Phys. Chem.* **1990**, *94*, 2963.
- (50) Nielsen, O. J.; Johnson, M. S.; Wallington, T. J.; Christensen, L. K.; Platz, J. *Int. J. Chem. Kinet.* **2002**, *34*, 283–291.
- (51) Scott, A. P.; Radom, L. *J. Phys. Chem.* **1996**, *100*, 16502.
- (52) Brown, S. T.; Rienstra-Kiracofe, J. C.; Schaefer, H. F. *J. Phys. Chem.* **1999**, *103*, 4065.
- (53) Adachi, H.; Basco, N.; James, D. G. *Int. J. Chem. Kinet.* **1979**, *11*, 1211.
- (54) Anastasi, C.; Waddington, D. J.; Woolley, A. *J. Chem. Soc. Faraday Trans. 1* **1983**, *79*, 505.
- (55) Munk, J.; Pagsberg, P.; Ratajczak, E.; Sillesen, A. *J. Phys. Chem.* **1986**, *90*, 2752.
- (56) Bauer, D.; Crowley, J. N.; Moortgat, G. K. *J. Photochem. Photobiol., A* **1992**, *65*, 329.
- (57) Fenter, F. F.; Catoire, V.; Lesclaux, R.; Lightfoot, P. D. *J. Phys. Chem.* **1993**, *97*, 3530.
- (58) Chettur, G.; Snelson, A. *J. Phys. Chem.* **1987**, *91*, 3483.
- (59) Mah, A.; Cabrera, J.; Nation, H.; Ramos, M.; Sharma, S.; Nickolaisen, S. L. *J. Phys. Chem. A* **2003**, *107*, 4354.
- (60) Adachi, H.; Basco, N. *Int. J. Chem. Kinet.* **1982**, *14*, 1125.
- (61) Zalyubovsky, S. J.; Glover, B. G.; Miller, T. A.; Hayes, C.; Merle, J. K.; Hadad, C. M. *J. Phys. Chem. A* **2005**, *109*, 1308.
- (62) Tarczay, G.; Zalyubovsky, S. J.; Miller, T. A. *Chem. Phys. Lett.* **2005**, *406*, 81.
- (63) Desain, J. D.; Klippenstein, S. J.; Miller, J. A.; Taatjes, C. A. *J. Phys. Chem. A* **2003**, *107*, 4415.
- (64) Burgess, A. R.; SenSharma, D. K.; White, M. J. D. *Adv. Mass Spectrom.* **1968**, *4*, 345.
- (65) Munk, J.; Pagsberg, P.; Ratajczak, E.; Sillesen, A. *Chem. Phys. Lett.* **1986**, *132*, 417.
- (66) Stark, M. S. *J. Am. Chem. Soc.* **2000**, *122*, 4162.
- (67) Chettur, G.; Snelson, A. *J. Phys. Chem.* **1987**, *91*, 913.
- (68) Clifford, E. P.; Wenthold, P. G.; Gareyev, R.; Lineberger, W. C.; DePuy, C. H.; Bierbaum, V. M.; Ellison, G. B. *J. Chem. Phys.* **1998**, *109*, 10293.
- (69) Parkes, D. A.; Donovan, R. J. *Chem. Phys. Lett.* **1975**, *36*, 211.
- (70) Chettur, G.; Snelson, A. *J. Phys. Chem.* **1987**, *91*, 5873.